Third-Order Optical Nonlinearity of Hexagonal Boron Nitride Atomic Layer

Tikaram Neupane *, Uma Poudyal, Bagher Tabibi, Felix Jaetae Seo *

Posted Date: 24 December 2024

doi: 10.20944/preprints202412.2015.v1

Keywords: Nonlinear Polarization; Two-photon and One-photon absorption; Free carrier absorption and dispersion

 doi:10.20944/preprints202412.2015.v1

Article

Third-Order Optical Nonlinearity of Hexagonal Boron Nitride Atomic Layer

Tikaram Neupane [1,*], Uma Poudyal [1], Bagher Tabibi [2] and Felix Jaetae Seo [2,*]

[1] Department of Chemistry and Physics, The University of North Carolina at Pembroke, Pembroke, NC 28372, USA
[2] Quantum Optics and NanoPhotonics, Department of Physics, Hampton University, Hampton, VA 23668, USA
* Correspondence: jaetae.seo@hamptonu.edu and tikaram.neupane@uncp.edu

Abstract: The third-order optical nonlinearity of hexagonal boron nitride (hBN) nanosheet was characterized by z-scan, I-scan, and spatial self-phase modulation (SSPM). The hBN nanosheets exhibited a positive nonlinear absorption or reverse saturable absorption (RSA) and its coefficient was estimated to be ~ 7.1 x 10^{-10} m/W via the open z-scan. The I-scan technique further verified the polarity of nonlinear absorption and the prospective application for laser safety (optical limiting) of the optical sensors from high-power lasers. It is found that the given hBN atomic layers could absorb up to ~22 % of incoming laser beam. In addition, the absence of a nonlinear refraction effect was observed using the closed z-scan and SSPM for a given excitation peak intensity. It implies that the free carrier-induced nonlinear absorption that diminishes the NLR signal via free-carrier dispersion. Acknowledgment: This work at HU is supported by ARO W911NF-15-1-0535 and NASA NNX15AQ03A.

Keywords: nonlinear polarization; two-photon and one-photon absorption; free carrier absorption and dispersion

1. Introduction

The hexagonal boron nitride nanosheets (h-BNNS) have garnered significant attention for a wide range of applications such as, optical power limiting, optical modulators, deep ultraviolet light emitters, laser, dielectrics layers, and solid-state thermal neutron detector, etc [1–8]. The h-BN has recently been subject to increased research interest due to the stable and softer structure that can resist oxidation at high-temperature applications [9]. It has strong bound excitons in the absorption spectrum in the UV region of both the monolayer and the bulk [10]. Therefore, the characterization of third-order nonlinearity using 532 nm (visible) and 800 nm(near-infrared) laser excitation is essentially important as the source of the single-photon at room temperature via the two-photon nonlinear process [11].

The third-order nonlinearity of hBN nanosheets are studied by z-scan, I-scan, and spatial self-phase modulation (SSPM) [12–16]. The z-scan techniques characterize the polarity and magnitude of nonlinear absorption (NLA) and nonlinear refraction (NLR) [17,18]. In NLA, one or more photons get absorbed in a single event depending on the material's bandgap energy compared to the excitation energy. These phenomena would change the beam transmittance through the medium due to the intensity-dependent absorption. On the other hand, NLR occurs in a medium when there is a change in either the net refractive index or the spatial distribution of the refractive index in the presence of external fields [13,14,19–23]. Also, the NLR can be characterized by spatial self-phase modulation (SSPM) which attracted extensive interest when Callen et al. observed the annular intensity distribution of a Gaussian laser beam passing through carbon disulfide in 1967 for the first time [24]. It is due to the intensity-dependent nonlinear refraction which differs along with the spatial intensity distribution of the laser beam. The coherent superposition of an optical wave of spatially varied phases causes the concentric diffraction rings of interference with constructive and destructive interferences [15,16,25]. In SSPM, the ring number is a function of laser input intensity, revealing a nonlinear refractive coefficient.

 doi:10.20944/preprints202412.2015.v1

The previous studies divulged the application of hBN on the optical power limiting using bare [3] and functional hBN nanosheets using z-scan and I-scan [4,5] with a 1064 nm excitation source. The single/few-layer in h-BN has recently opened new vistas for studying multiphoton absorption (MPA) in 2D materials [26]. Because of the wider bandgap materials, the excitation energy in the visible region could be non-resonant, resulting in reverse saturable absorption (RSA) through the two-photon and/or two-step excitation via the intermediate state. Also, the RSA phenomena occur if the excited state absorption cross-section (ESA) is larger than that of the ground-state absorption cross-section (GSA) [14]. Kumbhakar et al. [3] reported a strong two-photon absorption in few-layer h-BN sheets when exposed to nanosecond pulses of 1064 nm. It is due to the large transition dipole moment from the electronegativity difference between B and N atoms. Also, the huge range of magnitude of nonlinear absorption or/and two-photon absorption coefficient have been reported. For example, Ouyang et al. reported the nonlinear absorption coefficient of BN thin film in the order of ~ 10^{-7} m/W using a femtosecond laser of 400 nm wavelength [1]. However, Biswas et al. demonstrated the two-photon absorption with its coefficient in the order of 10^{-14} m/W using a nanosecond laser of 532 nm wavelength [5]. It infers that further study of NLA remains essential to enhance our understanding of the mechanisms of the nonlinear absorption process which may include two-photon absorption (TPA), free-carrier absorption (FCA), and free-carrier dispersion (FDA). Because of these free carriers mediated nonlinear absorption, the magnitude of the nonlinear refraction coefficient may be influenced. The measurement and analysis of these coefficients are crucial for evaluating the potential of BN in photonic applications. Therefore, this study focuses on the magnitude and polarity of NLA via open z-scan and its impact on nonlinear refraction through both closed z-scan and SSPM. Also, the coefficient of nonlinear absorption of hBN nanosheets in dispersion solution through the open z-scan was utilized to demonstrate the optical power limiting phenomena via the I-scan.

2. Materials and Methods

The hexagonal Boron Nitride nanosheets in ethanol/water solution were purchased from the Graphene Supermarket which was prepared by the liquid exfoliation method [27]. The concentration of nanosheet was ~5.4 mg/L which includes 1-5 monolayers with lateral sizes of 50-200 nm. The nonlinear absorption property of hBN was characterized by the open-aperture (OA) z-scan technique using a Gaussian beam. The Gaussian beam was prepared by two pin-hole method [28]. The excitation source for open z-scan was a pulsed laser at 532 nm, 10 Hz repetition rate, and ~6 ns temporal pulse width. The diameter of the Gaussian beam at the focusing lens was ~2.6 mm at FWHM. The effective focal length of the focusing lens for the z-scan was ~125 mm. The radius of the beam waist (w_o) at the focal point was ~16.2 um. The Rayleigh length ($z_o = kw_o^2/2$) was ~2.58 mm [17]. For the closed z-scan, the distance between the focal plane and the detector was 2.02 m. The finite aperture radius (r_a) in front of the detector was ~0.75 mm and the linear transmittance of the finite aperture was ~0.0049 which meets the closed z-scan condition [14,17]. The SSPM experiment was carried out using 800 nm wavelength of excitation source with 1.5-ps pulse width and 82 MHz repetition rate. The beam waist at the focal point was 40 μm and the Rayleigh length was ~ 1.1 cm. The measurement screen was placed at ~1 m away from the 1-cm quartz cuvette which contained the liquid suspension of atomic layers. The diffraction rings on the screen were captured by a CCD USB 2.0 camera (DCU223C, 1024 x 768 Resolution, Color, USB 2.0, Thorlabs, Inc.).

3. Results and Discussion

The linear absorption of hBN nanosheets (Figure 1) was measured by Agilent 8453 spectrometer. It shows the significant absorption is in the ultraviolet (UV) energy range. It implies that the hBN is transparent for visible to infrared (IR) wavelengths. To analyze the optical spectra of hBN nanoflakes, the plot of $(\alpha h\nu)^2$ vs $h\nu$ is presented in the inset of Figure 1. It satisfies the condition of $(\alpha h\nu)^2 \propto (h\nu - E_g)$ that estimates the optical band gap to be ~5.45eV [5,29]. Here α is an absorption coefficient calculated from the absorbance (A), $h\nu$ is the photon energy, and E_g is the bandgap of the materials. In the inset of Figure 1, the black dotted points are the experimental data abstracted from absorption, and a

 doi:10.20944/preprints202412.2015.v1

red dash line was drawn to find the point of intersection of it to the energy axis which estimates the bandgap of BN nanoflakes. Based on the estimated optical bandgap, the excitation source of 532 nm (~2.33 eV) and 800 nm (~1.55 eV) could be used as non-resonant excitation for the nonlinear optical excitations.

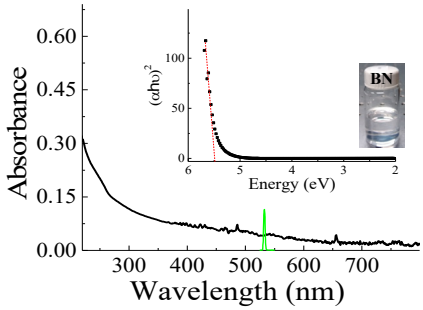

Figure 1. Absorption spectrum of hBN and inset figure estimates the optical bandgap.

The nonlinear absorption coefficient was estimated using the open z-scan technique. A Gaussian beam was prepared for this process with the help of the two-irises method [14]. The open z-scan technique displays the normalized transmittance as a function of z-position as shown in Figure 2. The experimental measurement revealed the reverse saturable absorption of positive nonlinearity for the different input peak intensities of 5.3 GW.cm^2, 3.0 GW/cm^2, 1.4 GW/cm^2, and 0.6 GW/cm^2. This implies that two-photon absorption or two-photon excitation may dominate the nonlinearity process. Fitting with the model [17], the nonlinear absorption coefficient of h-BN was estimated to be ~ 7.1 x 10^{-10} m/W.

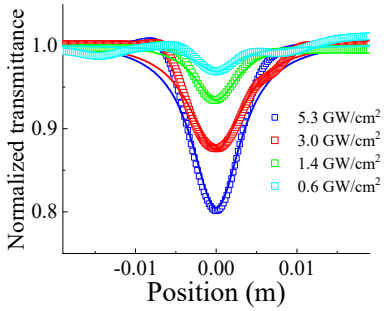

Figure 2. Nonlinear transmittance as a function of sample position along the z-axis for the different applied peak intensities with an open Z-scan.

The nonlinear effect requires an intense laser source which can significantly produce the heat effect. Thermal lensing initiated by high repetition rate lasers in z-scan experiments has been reported by various authors [30,31]. The light passing through the sample is partially absorbed by the sample and converted into heat. It is believed the time required to see a change in the material density as a consequence of acoustic waves is referred to as the acoustic transit time. It is the rise time of a thermal lens in an aqueous liquid which is denoted as $\tau = w_o/v_s$ [17] where w_o is the radius of the beam waist and $v_s \approx 1437$ m/s [32], is the velocity of sound in the water at room temperature. Consequently, we calculate τ to be approximately 11.27 ns, nearly double the pulse width of laser used, suggesting that the thermal diffusion time in water exceeds the pulse width [33]. This implies that non-uniform heating is induced by the 6 nm pulsed laser. Gnoli et al. [34] claimed thermal lensing accumulating over many laser pulses leads to flawed analysis and understanding of the nonlinear response, as well as a shifted origin. Another study showed that pulse duration, not the repetition rate, could also produce

 doi:10.20944/preprints202412.2015.v1

variations in the measurement as a result of acoustic thermal effects [35]. The same temperature gradient responsible for acoustic waves also generates a thermal lens which is often referred to as cumulative thermal effects. Thermal heating induced by a single laser pulse persists over some characteristic time t_c. Thus, the thermal effect increases whenever the time interval between consecutive laser pulses is shorter than t_c. In this case, a stationary lens is formed when a steady state is reached between the rate of heat generation and heat diffusion. If the laser repetition rate is much greater than $1/t_c$, the time scale of this cumulative process is given by $t_c = w_o^2/4D$, where D is the thermal diffusion coefficient (or diffusivity) of the material and w_o is the beam waist. At high repetition rates, the time between pulses is shorter than time t_c, and the sample does not have enough time to dissipate the heat from the previous pulse out of the beam diameter. This heat continues to build producing a thermal lens, eventually overtaking the electronic and molecular effects, and continuing to very high nonlinear absorption. Acoustic waves are more prevalent in the nanosecond and picosecond pulse width regimes [36]. Specifically, if the acoustic wave has enough time to completely traverse the beam profile, the thermal contribution can be attributed to accumulation of heat within the system.

In addition, the closed z-scan technique was used to characterize the nonlinear refraction. The normalized transmittance as a function of sample position doesn't display any significantly recognized peak and valley for the different peak intensities of 5.3 GW/cm^2 and 3.0 GW/cm^2 as shown in Figure 3. However, the normalized transmittance for 5.3 GW/cm^2 peak intensity seems to be a traceable nonlinear refraction signal compared with the intensity at 3.0 GW/cm^2. This work further characterizes the NLR coefficient through the spatial self-phase modulation technique.

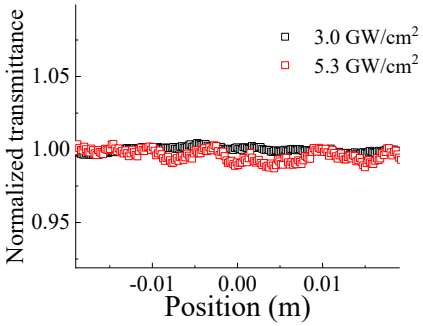

Figure 3. Nonlinear transmittance as a function of sample position along the z-axis for the different applied peak intensities with a closed Z-scan.

Moreover, the NLA of an optical sample could further be investigated by the I-scan technique where the intensity-dependent nonlinear transmittance was measured as a function of input peak intensity for a given stationary position in the z-axis as shown in Figure 4. It diminishes the laser target variation on the sample position along the z-axis which is beneficial for the inhomogeneous sample distribution in an aqueous solution [37]. Also, the sample is in a stationary position on the z-axis which prohibits passing through the focusing point that lowers the probability of sample damage due to the laser heat. I-scan demonstrated the normalized transmittance as a function of applied peak intensity, the total absorption being intensity-dependent and expressed mathematically as $\alpha(I) = \alpha_o + \beta I$ where α_o and β are the intrinsic linear and nonlinear absorption coefficients respectively. Figure 4 further verified the polarity of nonlinear absorption as nonlinear transmittance decreases with increased laser intensity. It implies that the total absorption of h-BN is decreased as the intensity increases for the intrinsic linear and nonlinear absorption coefficients. It shows that the nonlinear transmittance through the BN nanoflakes could decrease to ~78% of the incoming laser beam, which is suitable for the applications of optical power limiters.

 doi:10.20944/preprints202412.2015.v1

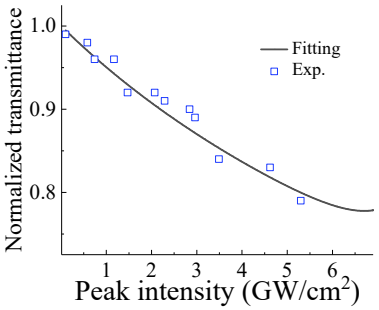

Figure 4: Nonlinear transmittance of h-BN nanosheets at the focal point of open Z-scan as a function of input peak intensity.

To investigate the nonlinear refraction further, the SSPM technique was deployed as described in the method and materials section. Figure 5a,b displayed the laser-induced diffraction rings of hBN in the liquid solution for the different peak intensities and different time durations of laser excitations respectively. The diffraction rings reveal that the nonlinear refraction phenomena don't change with the applied laser intensity. However, the nominal number (one- or two) of diffraction rings is seen as shown in Figure 5.

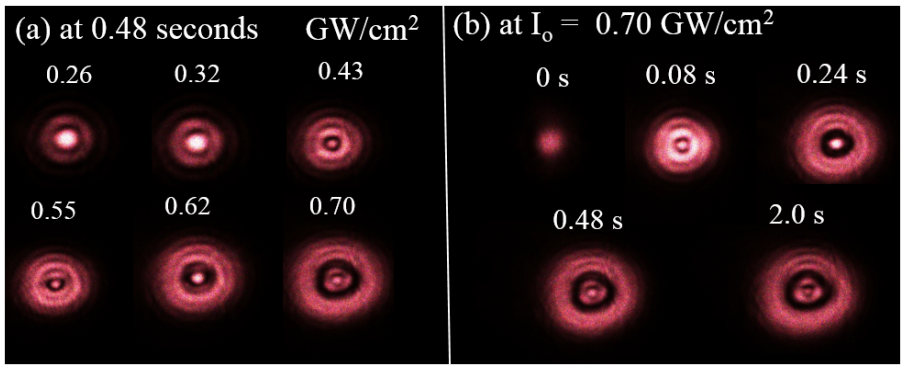

Figure 5. Diffraction patterns of SSPM at (a) different peak intensities and (b) at different time duration of laser excitations with the applied input intensity of ~0.7 GW/cm^2.

The optical kerr effect arises from the third-order nonlinear polarization through the oscillatory electric field, and the refractive index change depends linearly on the field intensity as $n(I) = n_o + n_2 I$. Nonlinear refraction occurs in a medium when there is a change in either the net refractive index or the spatial distribution of the refractive index in the presence of external fields. The closed z-scan characterizes the net refractive index change and a change of spatial distribution of the refractive index, associated with the SSPM. It is demonstrated that the strong presence of nonlinear absorption in h-BN may impact the nonlinear refraction through the free-carrier absorption (FCA) and free-carrier dispersion (FCD) during the excitation process [38–41]. Yan et al., [38] described the free carrier induced nonlinear absorption through the TPA, FCA, and FCD. The FCD-induced phase shift has a sign opposite to that of the Kerr effect, which results in the reduction of the total magnitude of the nonlinear refraction signal during the nonlinear process. The nonlinear effect is supposed to be enhanced if only TPA is considered. However, the nonlinear refraction properties remain almost constant because of the presence of possible free carrier absorption. Therefore, even after increasing the input laser intensity, the number of rings may not increase which contradicts the general SSPM phenomenon.

 doi:10.20944/preprints202412.2015.v1

4. Conclusions

The third-order nonlinearity of hexagonal Boron Nitride nanosheets was characterized by open z-scan, I-scan, and SSPM. The open Z-scan and I-scan techniques were conducted with the laser excitation at 532 nm, 10 Hz repetition rate, and ~6 ns pulse width. The open Z-scan revealed the positive nonlinear absorption or reverse saturable absorption, and its coefficient was estimated to be ~ 7.1 x 10^{-10} m/W. Because of the wide bandgap, the absorption process may include two-photon or two-step through the virtual intermediate state. It could be inferred that the hBN has a larger excited state absorption cross-session (ESA) than the ground state absorption cross-section (GSA). However, the nonlinear refraction effect was not significantly observed using the closed z-scan and SSPM for a given excitation peak intensity. It might be the effect of free carrier-induced nonlinear absorption. The free carrier-induced NLA including FCD reduces the magnitude of the NLR signal. Furthermore, the polarity of NLA and its impact on the total absorption was reexamined by the I-scan technique. Finally, the hBN atomic layers could absorb up to ~22 % of the incoming laser beam which might be applicable for the protection of optical sensors from high-power lasers.

Author Contributions: Conceptualization, Jaetae Seo; methodology, Tikaram Neupane; formal analysis, Tikaram Neupane; resources, Jaetae Seo; data curation, Tikaram Neupane.; writing—original draft preparation, Tikaram Neupane; writing—review and suggestion, Jaetae Seo, and Bagher Tabibi; visualization, Tikaram Neupane; supervision, Jaetae Seo and Bagher Tabibi; funding acquisition, Jaetae Seo. All authors have read and agreed to the published version of the manuscript.

Acknowledgments: The research at HU was funded by ARO W911NF-15-1-0535 and NASA NNX15AQ03A.

Conflicts of Interest: The authors declare no conflict of interest.

References

1. lavin, N. R.; Jespersen, M. L.; Check, M. H.; Hu, J. J.; Hilton, A. M.; Fisher, T. S.; Voevodin, A. A. Synthesis of few-layer large area hexagonal-boron nitride by pulsed laser deposition. *Thin Solid Films* **2014**, 572, 245–250.
2. umbhakar, P.; Kole, A. K.; Tiwary, C. S.; Biswas, S.; Vinod, S.; Tijerina, J. T.; Chatterjee, U.; Ajayan, P.M. Nonlinear Optical Properties and Temperature-Dependent UV–Vis Absorption and Photoluminescence Emission in 2D Hexagonal Boron Nitride Nanosheets. *Adv. Optical Mater*. **2015**, 3, 828–835.
3. hao, G.; Zhang, F.; Wu, Y.; Hao, X.; Wang, Z.; Xu, X. One-Step Exfoliation and Hydroxylation of Boron Nitride Nanosheets with Enhanced Optical Limiting Performance. *Adv. Optical Mater*. **2016**, 4, 141–146.
4. iswas, S.; Tiwary, C. S.; Vinod, S.; Kole, A. K.; Chatterjee, U.; Kumbhakar, P.; Ajayan, P. M. Nonlinear Optical Properties and Temperature-Dependent Photoluminescence in hBN-GO Heterostructure 2D Material. *J. Phys. Chem. C* **2017**, 121, 8060–8069.
5. oan, T. C.; Majety, S.; Grenadier, S.; Li, J.; Lin, J. Y.; Jiang, H. X. Hexagonal boron nitride thin film thermal neutron detectors with high energy resolution of the reaction products. *Nucl. Instrum. Meth. Phys. Res. Sect. A* **2015**, 783, 121–127.
6. ersisyan, H. H.; Lee, T. H.; Lee, K. H.; An, Y. S.; Lee, J. S.; Lee, J. H. Few-atomic-layer boron nitride nanosheets synthesized in solid thermal waves. *RSC Advances* **2015**, 5, 8579–8584.
7. su, A.; Han, W.; Yong, C. S.; Maily, B.; Xu, Z.; Lili, Y.; Yumeng, S.; Yi, H. L.; Dubey, M.; Ki, K. K.; Jing, K.; Palacios, T. Large-Area 2-D Electronics: Materials, Technology, and Devices. *Proc. IEEE* **2013**, 101, 1638–1652.
8. iu, Z.; Gong, Y.; Zhou, W.; Ma, L.; Yu, J.; Idrobo, J. C.; Jung, J.; MacDonald, A. H.; Vajtai, R.; Lou, J.; Ajayan, P. M. Ultrathin high-temperature oxidation-resistant coatings of hexagonal boron nitride. *Nature Comm*. **2013**, 4, 2541.
9. ttaccalite, C.; Grüning, M.; Amara, H.; Latil, S.; Ducastelle, F. Two-photon absorption in two-dimensional materials: The case of hexagonal boron nitride. *Phys, Rev. B* **2018**, 98, 165126.
10. chell, A. W.; Tran, T. T.; Takashima, H.; Takeuchi, S.; Aharonovich, I. Nonlinear excitation of quantum emitters in hexagonal boron nitride multiplayers. *APL Photonics* **2016**, 1, 091302.

 doi:10.20944/preprints202412.2015.v1

11. . Wang, G.; Zhang, S.; Zhang X.; Zhang, L.; Cheng, Y.; Fox, D.; Zhang, H.; Coleman, J. N.; Blau, W. J.; Wang, J. Tunable nonlinear refractive index of two-dimensional MoS_2, WS_2, and $MoSe_2$ nanosheet dispersions. *Photon. Res*. **2015**, 3, A51–A55.
12. oyd, R. W. Nonlinear Optics, Academic Press, Elsevier, USA, **2003**.
13. . Neupane, T.; Yu, Y.; Rice, Q.; Tabibi, B.; Seo, F. J. Third-order optical nonlinearity of tungsten disulfide atomic layer with resonant excitation. *Optical materials* **2019**, 96, 109271.
14. . Wang, W.; Wu, Y.; Wu, Q.; Hua, J.; Zhao, J. Coherent Nonlinear Optical Response Spatial Self-Phase Modulation in $MoSe_2$ Nano-Sheets. *Sci. Rep*. **2016**, 6, 22072.
15. . Durbin, S. D.; Arakelian, S. M.; Shen, Y. R. Laser-induced diffraction rings from a nematic-liquid-crystal film. *Opt. Lett*. **1981**, 6, 411–413.
16. ahae, M. S.; Said, A. A.; Wei, T. H.; Hagan, D. J.; Van Stryland, E. W. Sensitive Measurement of Optical Nonlinearities Using a Single Beam. IEEE J. *Quantum Electron*, **1990**, 26, 760–769.
17. eupane, T.; Rice, Q.; Jung,S.; Tabibi, B.; Seo, F. J. Cubic Nonlinearity of Molybdenum Disulfide Nanoflakes. *J. Nanosci. Nanotechnol* **2020**, 20, 4373–4375.
18. eupane, T.; Yu, Y.; Rice, Q.; Tabibi, B.; Seo, F. J. Third-order optical nonlinearity of tungsten disulfide atomic layer with resonant excitation. *Optical materials* **2019**, 96, 109271.
19. eo, J. T.; Yang, Q.; Kim, W. J.; Heo, J.; Ma, S. M.; Austin, J.; Yun, W.S.; Jung, S.S.; Han, S.W.; Tabibi, B.; Temple, D. Optical nonlinearities of Au nanoparticles and Au/Ag coreshells. *Optics Letters* **2009**, 34, 307–309.
20. a, S. M.; Seo, J. T.; Yang, Q.; Battle, R.; Brown, H.; Lee, K.; Creekmore, L.; Jackson, A.; Skyles, T.; Tabibi, B. Third-Order Nonlinear Susceptibility and Hyperpolarizability of CdSe Nanocrystals with Femtosecond Excitation. *J. Korean Phys. Soc*. **2006**, 48, 1379.
21. . Neupane, T.; Tabibi, B.; Seo, F. J. Spatial self-phase Modulation in WS_2 and MoS_2 Atomic Layer. *Optical Materials Express* **2020**, 10, 831–842.
22. . Neupane, T.; Wang, H.; Yu, W. W.; Tabibi, B.; Seo, F. J. Second-order hyperpolarizability and all-optical switching of intensity-modulated spatial self-phase modulation in $CsPbBr_{1.5}I_{1.5}$ perovskite quantum dot. *Optics and Laser Technology* **2021**, 140, 107090.
23. . Callen, W. R.; Huth, B. G.; Pantell, R. H. Optical Patterns of Thermally Self-Defocused Light. *Appl. Phys. Lett*. **1967**, 11, 103–105.
24. . Neupane, T.; Tabibi, B.; Kim, K-J.; Seo, F. J. "Spatial Self-Phase Modulation in Graphene Oxide Monolayer." *Crystal* **2023**, 13, 271.
25. urlbut, W.C.; Lee, Y. S.; Vodopyanov, K. L.; Kuo, P. S.; Fejer, M. M. Multiphoton absorption and nonlinear refraction of GaAs in the mid-infrared. *Optics Letter* **2007**, 32, 668.
26. oleman, J. N.; Khan, U.; Young, K.; Gaucher, A.; De, S.; Smith, R. J.; Shvets, I. V.; Arora, S. K.; Stanton, G.; Kim, H.; Lee, K.; Kim, G. T.; Duesberg, G. S.; Hallam, T.; Boland, J. J.; Wang, J. J.; Donegan, J. F.; Grunlan, J. C.; Moriarty, G.; Shmeliov, A.; Nicholls, R. J.; Perkins, J. M.; Grieveson, E. M.; Theuwissen, K.; Mccomb, D. W.; Nellist, P. D.; Nicolosi, V. Two-Dimensional Nanosheets Produced by Liquid Exfoliation of Layered Materials, *Science* **2011**, 331, 568-571.
27. eupane, T.; Poudyal, U.; Tabibi, B.; Kim, K-J.; Seo, F. J. "Cubic Nonlinearity of Graphene Oxide Monolayer." *materials* **2023**, 16, 6664.
28. ox, M. Optical properties of solids, second edition Oxford University press, page 81 (2010).
29. . Nalda, R. de; Coso, R. del; Requejo-Isidro, J.; Olivares, J.; Suarez-Garcia, A.; Solis, J.; Afonso, C. N. Limits to the determination of the nonlinear refractive index by the Z-scan method. *J. Opt. Soc. Am*. B **2002**, 19, 289.
30. . Falconieri, M. Salvetti, G. Simultaneous measurement of pure-optical and thermo-optical nonlinearities induced by high- repetition-rate, femtosecond laser pulses: application to CS_2. *Appl. Phys*. B **1999**, 69, 133.
31. . Martin, K.; Spinks, D. Measurement of the speed of sound in ethanol/water mixture. *Ultrasound Med. Biol*. **2001**, 27, 289-291.
32. . Khabibullin, V. R.; Usoltseva, L. O.; Galkina, P. A.; Galimova, V. R.; Volkov, D. S.; Mikheev, I. V.; Proskurnin, M. A. Measurement Precision and Thermal and Absorption Properties of Nanostructure in Aqueous Solutions by Transient and Steady-State Thermal-Lens Spectrometry. *Phys. chem*. **2023**, 3, 156–197.

 doi:10.20944/preprints202412.2015.v1

33. . Gnoli, A.; Razzari, L.; M. Righini, M. Z-scan measurements using high repetition rate lasers: how to manage thermal effects. *Opt. Express* **2005**, 13, 7976–7981.
34. . Ganeev, R. A.; Ryasnyansky, A. I.; Baba, M.; Suzuki, M.; Ishizawa, N.; Turu, M.; Sakakibara, S.; Kuroda, H. Nonlinear refraction in CS2. *Appl. Phys. B* **2004**, 78, 433–438.
35. . Burkins, P.; Kuis, R.; Basaldua, I.; Johnson, A. M.; Swaminathan, S. R.; Zhang, D.; Trivedi S. Thermally Managed Z-scan methods investigation of the size-dependent nonlinearity of graphene oxide in various solvents. *J. Opt. Soc. Am. B* **2016**, 33, 2395–2401.
36. ang, Q.; Seo, J. T.; Creekmore, S.; Temple, D.; Mott, A.; Min, N.; Yoo, K.; Kim, S. Y.; Jung, S. Distortions in Z-scan spectroscopy. *Appl. Phys. Lett* **2003**, 82, 19–21.
37. . Yin, L.; Agrawal, G. P. Impact of two-photon absorption on self-phase modulation in silicon waveguides. *Optics Letters* **2007**, 32, 2031–2033
38. . Ulmer, T. G.; Tan, R. K.; Zhou Z.; Ralph, S. E.; Kenan, R. P.; Verber, C. M. Two-photon absorption-induced self-phase modulation in GaAs-AlGaAs waveguides for surface-emitted second-harmonic generation. *Optics Letters* **1999**, 24, 756–758.
39. . Huy, M. C. P.; Baron, A.; Lebrun, B.; Frey, R.; Delay, P. Characterization of self-phase modulation in liquid filled hollow photonic bandgaps fibers. *J. Opt. Soc. Am. B* **2010**, 27, 1886–1893.
40. . Dekker, R.; Driessen, A.; Wahlbrink, T.; Moormann, C.; Niehusmann, J.; Forst, M. Ultrafast Kerr-induced all-optical wavelength conversion in silicon waveguides using 1.55 μm femtoseconds pulses. *Optics Express* **2006**, 14, 8336–8346.